

# Nitride Formation in Synthesis of Titanium Aluminide Matrix Composite Coatings by Reactive RF Plasma Spraying

Yoshiki Tsunekawa, Makoto Hiromura, and Masahiro Okumiya

(Submitted 14 January 1999; in revised form 6 December 1999)

This paper presents an *in situ* process to form intermetallic matrix composite coatings by reactive radio frequency (RF) plasma spraying with premixed elemental powder. The typical splat morphology of impinged titanium droplets on a stainless steel substrate is a disk with an outer peripheral fringe. If the supplied titanium powder size becomes finer or the nitrogen partial pressure in the plasma gas increases, splats containing prominent asperities with a smaller flattening ratio appear along with the plain disk type. An increase in nitrogen content is detected in all the splats sprayed with finer titanium powder and/or higher nitrogen partial pressure. The splats containing prominent asperities, which correspond to TiN, are twice as high in nitrogen content than the plain disk type.

Aluminum splats are also classified into two categories: a disk type with an irregular outer periphery and a seminodular type. Oxygen exists on the splat surfaces, on which there are nitrogen concentrated areas corresponding to AlN. Consequently, the nitride formation proceeds on titanium and aluminum droplets during the flight as well as on the substrate. If the substrate temperature is higher than 873 K just before spraying with premixed titanium and aluminum powder, the formation of TiAl and Ti<sub>2</sub>AlN proceeds on the substrate because of negligible mutual collisions during the flight. Titanium aluminide matrix *in situ* composites sprayed with premixed titanium and aluminum powder contain more nitrides than those sprayed with TiAl compound powder, because of the higher nitrogen absorption in titanium and aluminum droplets that results in an exothermic reaction.

**Keywords** reactive plasma spraying, premixed elemental powder, reaction synthesis, nitride, intermetallic matrix composite, splat morphology

## 1. Introduction

Low density titanium aluminides exhibit superior high-temperature strength and oxidation resistance. However, the hardness and wear resistance should be improved for high load bearing applications requiring wear resistance at elevated temperatures. Production of intermetallic matrix composites is an approach to overcome the above difficulties. The reaction synthesis processes can be applied to the production of TiAl matrix composites, instead of conventional casting processes. They were successfully fabricated from elemental powders of titanium and aluminum through the addition of SiC<sup>[1]</sup> or TiB<sub>2</sub> particles.<sup>[2,3]</sup> As well as the above processes, there is a novel fabrication method for intermetallic matrix composites, in which *in situ* reinforcements are formed during the process without preparing any fibers or particles. As a typical example, electrical discharge machining was used to synthesize TiC/TiAl *in situ* composite layers on aluminum alloy substrates using an electrode of titanium powder formed as a green compact.<sup>[4]</sup>

Plasma spraying has been applied to fabricate compositionally graded coatings such as thermal barrier coatings<sup>[5,6]</sup> and com-

posite coatings.<sup>[7-11]</sup> The elemental steps in the coating process of reactive plasma spraying are quite complex, so that there are some uncertainties. For example, it is not clear whether the nitriding reaction takes place on droplets during flight in the nitrogen plasma flame or after impingement on a substrate. Such ambiguity is reflected in the structural control of *in situ* composite coatings. Compared with direct current (DC) plasma spraying, a radio frequency plasma flame is characterized by high temperature and low velocity. Consequently, it is suitable to control the reaction synthesis of both intermetallic matrices and *in situ* reinforcements.

This study is aimed at developing the formation process of titanium aluminide matrix *in situ* composite coatings containing nitrides by reactive RF plasma spraying. The nitride formation in molten titanium and aluminum droplets during the flight is examined along with the deposition on a substrate. Then, the effect of droplet size and nitrogen partial pressure in the plasma gas on the nitride formation is discussed. Titanium aluminide matrix *in situ* composite coatings were fabricated with premixed titanium and aluminum powder and TiAl compound powder, in which the effect of the exothermic reaction of TiAl on the nitride formation is also examined.

## 2. Experimental

### 2.1 Splat collection

In order to examine the titanium, aluminum, and TiAl splat morphology, several tens of molten droplets having nearly equal

Yoshiki Tsunekawa, Makoto Hiromura, and Masahiro Okumiya, Toyota Technological Institute, Hisakata, Tempaku, Nagoya 468-8511, Japan.

temperature and velocity just before impinging were collected on a substrate by passing through a fixed slit with a circular hole of 10 mm in diameter and a moving graphite shutter with a 15 mm diameter hole.<sup>[12]</sup> The shutter system was installed above the substrate, as shown in Fig. 1.

Elemental powders, titanium (99.8 mass% in purity), aluminum (99.7 mass%) and TiAl (99.4 mass%), were sieved to obtain particles in the size ranges of 10 to 20, 20 to 25, 25 to 32, 32 to 38, and 38 to 45  $\mu\text{m}$  in diameter. Stainless steel (SUS304) of  $30 \times 30 \times 5$  mm in size with a mirror finished surface was used as a substrate. The substrate temperature was continuously recorded by inserting a thermocouple into the center, 2.5 mm apart from the substrate surface. The atmosphere in the vacuum chamber was maintained at 26.7 kPa during the splat collection. The standard spray parameters are listed in Table 1.

The splats were collected on the substrate by opening the graphite shutter. There was no rise in substrate temperature, which was approximately 318 K during the splat collection. The titanium, aluminum, and TiAl splats were then examined: the element distribution by electron probe microanalysis (EPMA) and Auger electron spectroscopy (AES) and the splat morphology observation by scanning electron microscopy (SEM) and atomic force microscopy (AFM). The phase identification of splats was also performed by X-ray diffractometry (XRD) with  $\text{Co } K_{\alpha}$  radiation.

**Table 1** Spray parameters in reactive RF plasma spraying

RF power	10(kW)
Plasma gas flow	Ar/N <sub>2</sub> /H <sub>2</sub> : 233/(0–67)/2 ( $\times 10^{-6}$ m <sup>3</sup> /s)
Sheath gas flow	Ar/He: (533–600)/83 ( $\times 10^{-6}$ m <sup>3</sup> /s)
Carrier gas flow	Ar: 37 ( $\times 10^{-6}$ m <sup>3</sup> /s)
Chamber pressure	26.7 (kPa)
Spray materials	Ti, Al, TiAl compound, premixed Ti/Al
Substrate	Stainless steel (SUS304)

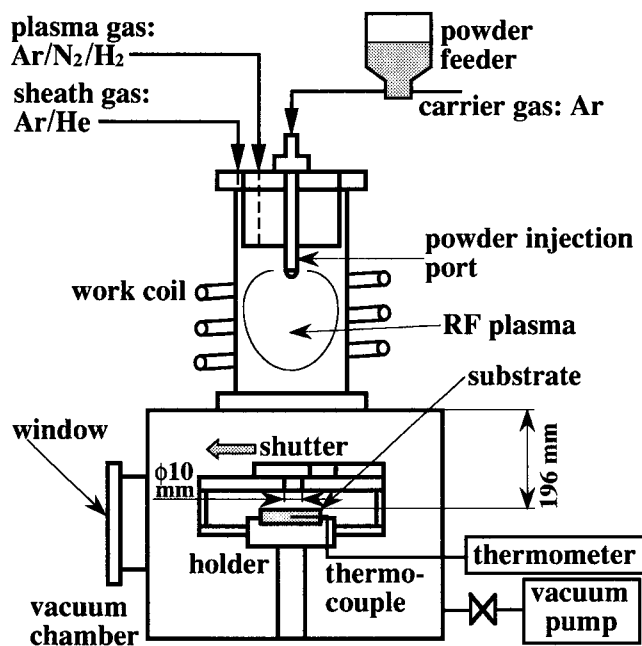


**Fig. 1** Schematic diagram of the reactive RF plasma spray system.

## 2.2 Formation of In Situ Composite Coatings

Premixed powder of 50 at.% Ti and 50 at.% Al with various particle sizes and TiAl compound powder were supplied as a spray material for the direct fabrication of *in situ* composite coatings by reactive RF plasma spraying with nitrogen mixed plasma gas.

The sprayed coatings were fabricated by the RF plasma spray system of Fig. 1, however, without using the shutter system. The substrate temperature was continuously recorded by inserting a thermocouple into the center 2.5 mm from the substrate surface. Stainless steel (SUS304) was used as a substrate, but its surface was blasted using alumina grit just before spraying, instead of the mirror finishing for the splat collection. The standard spray parameters for the coating formation are the same as shown in Table 1.

Spectroscopic analyses of nitrogen content in coatings, optical microscopy, and SEM observations on the cross section of coatings, analyses of XRD with  $\text{Co } K_{\alpha}$  radiation and EPMA were then carried out to characterize the coatings.

## 3. Results and Discussion

### 3.1 Flight Velocity of Droplets

The flight velocity of droplets just before impingement on a substrate affects the residence time in the plasma flame and the flattening ratio of splats. The flight velocities of molten titanium, aluminum, and TiAl droplets were measured in nitrogen ( $17 \times 10^{-6}$  m<sup>3</sup>/s) mixed plasma flame by using photographs of a trajectory of flight droplets taken at a shutter speed of 0.5 ms. The average flight velocity of titanium droplets is shown in Fig. 2 as a function of average particle size, as well as the velocities of aluminum and TiAl droplets with a constant particle size range of 38 to 45  $\mu\text{m}$ . The velocity of titanium droplets decreases as the particle size increases. Comparing the velocities of aluminum and TiAl with those of titanium, aluminum droplets with lower liquid density ( $\rho_{\text{Al}} = 2.385$  Mg/m<sup>3</sup> at melting point<sup>[13]</sup>) are 5 m/s faster than titanium ( $\rho_{\text{Ti}} = 4.11$  Mg/m<sup>3</sup> at melting point<sup>[13]</sup>) droplets of particle size of approximately

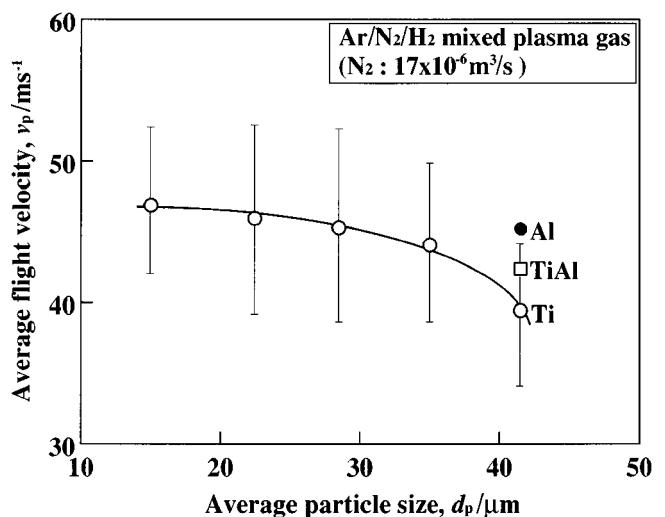


**Fig. 2** Change in average flight velocity of molten titanium droplets as a function of average particle size.

41.5  $\mu\text{m}$ . The flight velocity of droplets with smaller volume and lower liquid density becomes faster in a nitrogen mixed plasma flame because the droplets can rapidly approach the plasma flame velocity. The flight velocity also decreases with an increase in nitrogen partial pressure in the plasma gas. Hence, the residence time in the nitrogen mixed plasma flame is approximately 7 ms, which is much longer than that in the DC plasma flame at low pressure.<sup>[14]</sup>

### 3.2 Splat Morphology

In order to examine the splat morphology quantitatively, AFM observations were carried out, as shown in Fig. 3(a) of a typical titanium splat, which was formed in a nitrogen ( $17 \times 10^{-6} \text{ m}^3/\text{s}$ ) mixed plasma flame using particles with 32 to 38  $\mu\text{m}$  diameter. The splats are nearly circular with an outer peripheral fringe. The maximum fringe height is 3.44  $\mu\text{m}$  (Fig. 3b). The central flat area on the splat is approximately 2  $\mu\text{m}$ , which indicates that the droplets evaporate during flight in the high-temperature plasma flame by comparison of splat and droplet volumes, although the residence time is extremely short.

The splat appearances of aluminum and TiAl observed by SEM are also shown in Fig. 4. A splash phenomenon is not observed on the impinged titanium, aluminum, and TiAl splats sprayed under the parameters of Table 1. Disk-type aluminum splats (Fig. 4a) are characterized by an irregular outer periphery, although 70% of aluminum splats are a seminodular type (Fig. 4b). The splat morphology of TiAl is almost the same as that of titanium: in addition to a plain disk type (Fig. 4c), there are small amounts (10%) of disk-type TiAl splats with prominent asperities in the central flat area (Fig. 4d).

The flattening ratio of splats using particles of 32 to 38  $\mu\text{m}$  diameter, which had impinged, flattened, and solidified on the

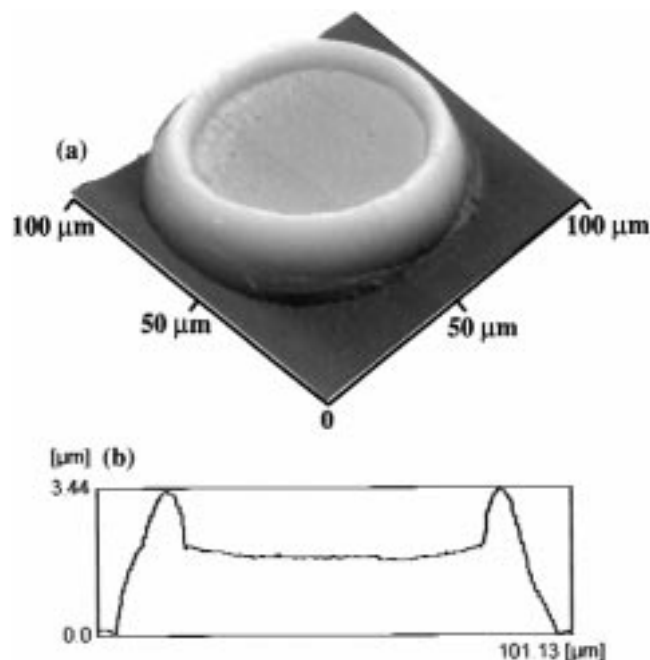


**Fig. 3** Typical AFM image showing (a) splat morphology and (b) cross-sectional profile of titanium splat (particle size: 32 to 38  $\mu\text{m}$ , added  $\text{N}_2$ :  $17 \times 10^{-6} \text{ m}^3/\text{s}$ ).

substrate, was calculated from the measured splat diameter and the average droplet diameter. The flattening ratios of disk-type aluminum and TiAl splats,  $2.4 \pm 0.3$ , are approximately the same as  $2.34 \pm 0.3$  for titanium splats. In contrast, the flattening ratio of seminodular-type aluminum splats is  $1.9 \pm 0.2$ . The characterized disk-type TiAl and titanium splats with prominent asperities show smaller flattening ratios of 1.4 to  $1.8 \pm 0.2$  than those of a plain disk type.

### 3.3 Nitride Formation on Droplets during the Flight

The nitrogen absorption and nitride formation on titanium, aluminum, and TiAl splats, which had been sprayed with nitrogen mixed plasma gas using the 32 to 38  $\mu\text{m}$  diameter particles, were examined by EPMA, as shown in Fig. 5(a) and (c) for the splats containing prominent asperities and Fig. 5(b) for the seminodular-type aluminum splat. The  $\text{N } K_{\alpha}$  intensity was corrected with respect to pure TiN and titanium standards. The intensity distributions of the  $\text{Ti } K_{\alpha}$  and  $\text{N } K_{\alpha}$  peaks of the titanium splat are consistent and the existence of nitrogen is recognized on the titanium splats, as well as on aluminum and TiAl splats. There are also nitrogen-concentrated areas on aluminum splats, whereas such features are not observed on aluminum splats sprayed with a DC plasma at low pressure.<sup>[14]</sup>

Based on the examination of depth profiles of Auger electron intensity on titanium and aluminum splats, the existence of nitrogen is recognized in the thickness direction of the titanium splat. In contrast, plain disk-type aluminum splats have no N intensity on the depth profile, although oxygen exists at the splat surface. Oxygen may be absorbed during the flight or exist on the particle surface originally. However, 70% of aluminum splats, which are seminodular type in appearance (Fig. 4b), have nitrogen concentrated areas, as shown in Fig. 5b. AlN formation,

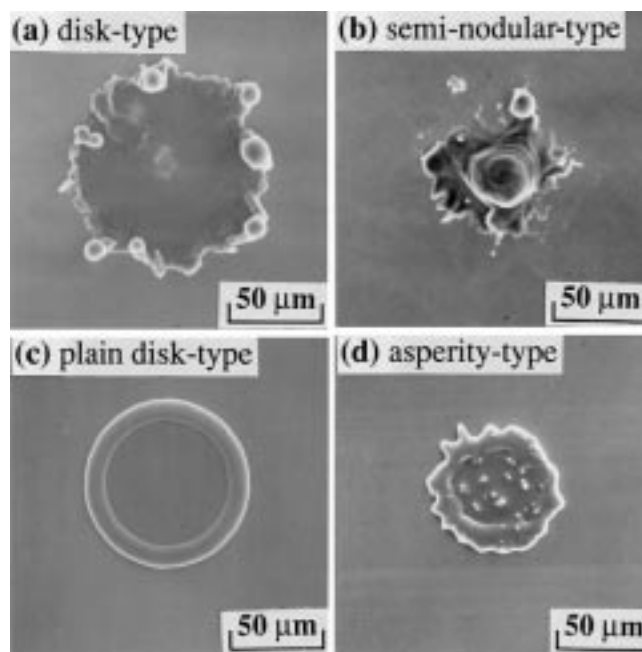


**Fig. 4** Splat morphology of (a) and (b) aluminum and (c) and (d) TiAl compound observed by SEM (particle size: 32 to 38  $\mu\text{m}$ , added  $\text{N}_2$ :  $17 \times 10^{-6} \text{ m}^3/\text{s}$ ).

which has occurred in flight within the nitrogen mixed plasma flame, is also clearly recognized in the XRD pattern of the aluminum splats.

However, there are no diffraction peaks from nitrides in the XRD patterns of titanium and TiAl splats, since the amount of nitrides formed or the volume regarding the diffraction is so small that they cannot be detected. The nitride formation of TiN can be recognized on the titanium and TiAl splats with prominent asperities, which were sprayed with finer particles, instead of 32 to 38  $\mu\text{m}$  in diameter.

### 3.4 Effects of Droplet Size and Added Nitrogen on the Nitride Formation

The effect of droplet size on the splat morphology was examined by supplying titanium powders with different sizes, as shown in Fig. 6. With nitrogen ( $17 \times 10^{-6} \text{ m}^3/\text{s}$ ) mixed plasma

gas, two types of splats are detected: one is a plain disk type, and the other is a disk-type splat with prominent asperities in the central flat area. The number fraction ( $R_n$ ) is defined as a fraction of plain disk-type splats or splats containing prominent asperities to the collected total splat number (>100). The number fraction of splats with prominent asperities increases as the particle size becomes smaller, because small particles readily absorb nitrogen due to the large specific surface. The flattening ratio of splats with prominent asperities of TiN is rather small compared with that of plain disk-type splats. Although the flattening ratio of splats with prominent asperities does not change much with respect to different particle sizes, the flattening ratio of plain disk-type splats decreases from  $2.3 \pm 0.3$  to  $1.9 \pm 0.3$  as the particle size becomes smaller.

The intensity ratio of  $\text{N } K_\alpha$  on a splat surface to that on the pure TiN standard was measured by spot analysis of EPMA (Fig. 7). The intensity ratio on prominent asperities increases with particles



Fig. 5 Typical  $\text{N } K_\alpha$  images of EPMA of (a) titanium, (b) aluminum, and (c) TiAl compound splat (particle size: 32 to 38  $\mu\text{m}$ , added  $\text{N}_2$ :  $17 \times 10^{-6} \text{ m}^3/\text{s}$ ).

	$10 < d_p < 20 \mu\text{m}$	$20 < d_p < 25 \mu\text{m}$	$25 < d_p < 32 \mu\text{m}$	$32 < d_p < 38 \mu\text{m}$	$38 < d_p < 45 \mu\text{m}$
plain disk-type					
	$R_n=0.24$	$R_n=0.66$	$R_n=0.92$	$R_n=0.98$	$R_n=1.0$
prominent dot-type					
	$R_n=0.76$	$R_n=0.34$	$R_n=0.08$	$R_n=0.02$	$R_n=0$

Fig. 6 SEM micrographs showing titanium splat morphology sprayed with different particle sizes (added  $\text{N}_2$ :  $17 \times 10^{-6} \text{ m}^3/\text{s}$ ).

less than  $32\ \mu\text{m}$ ; the prominent asperities exhibit approximately two times higher  $N\ K_{\alpha}$  intensity than that on the flat area. The  $N\ K_{\alpha}$  intensity ratio decreases as the particle size increases, because the nitrogen absorption from droplet surfaces becomes more difficult owing to the decreased specific surface and the finer size of the TiN asperities. Consequently, the fine droplets are more suitable for the nitride formation, although it is difficult to feed fine particles during RF plasma spraying.

The effect of the nitrogen ratio in the plasma gas on the splat morphology was also examined by supplying titanium powder  $32$  to  $38\ \mu\text{m}$  in size (Fig. 8). The disk-type splats with prominent asperities in the central flat area similar to Fig. 6 can be detected. The high concentration nitrogen plasma gas has the same influ-

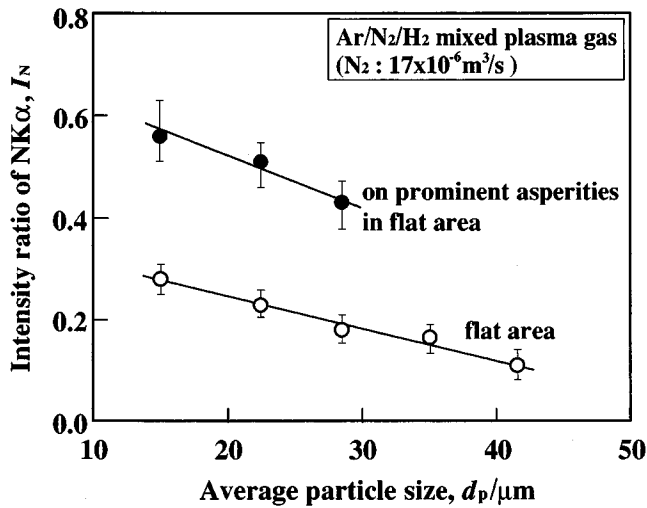


Fig. 7 Intensity ratio of  $N\ K_{\alpha}$  on titanium splats to that on TiN as a function of average particle size.

ence as fine particles on the splat morphology. The flattening ratio of splats containing TiN asperities also becomes smaller compared with that of plain disk-type splats. At mixed nitrogen of  $50 \times 10^{-6}\ \text{m}^3/\text{s}$ , nearly 40% of titanium splats become a prominent asperity type with a small flattening ratio.

The splats with prominent asperities appear with mixed  $N_2$  higher than  $17 \times 10^{-6}\ \text{m}^3/\text{s}$ ; the prominent asperities show higher  $N\ K_{\alpha}$  intensity, as shown in Fig. 9. The  $N\ K_{\alpha}$  intensity ratio increases as the mixed nitrogen increases, because the nitrogen absorption from atmosphere is easier under high nitrogen partial pressure. Consequently, the plasma flame highly mixed with nitrogen is more suitable for the nitride formation.

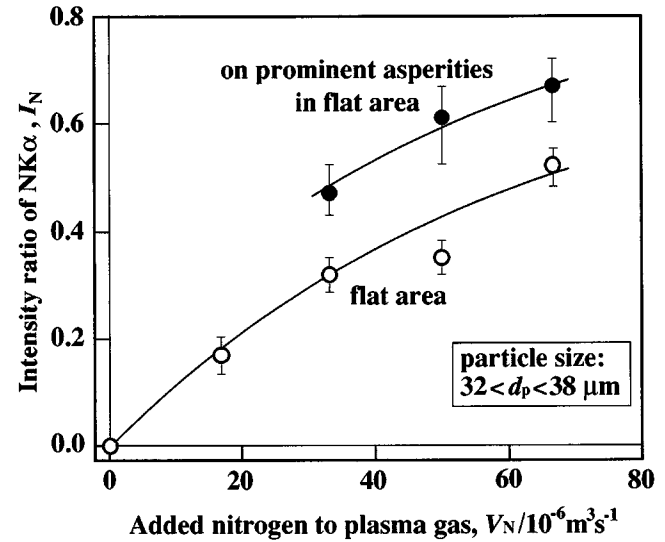


Fig. 9 Intensity ratio of  $N\ K_{\alpha}$  on titanium splats to that on TiN as a function of added nitrogen to plasma gas.

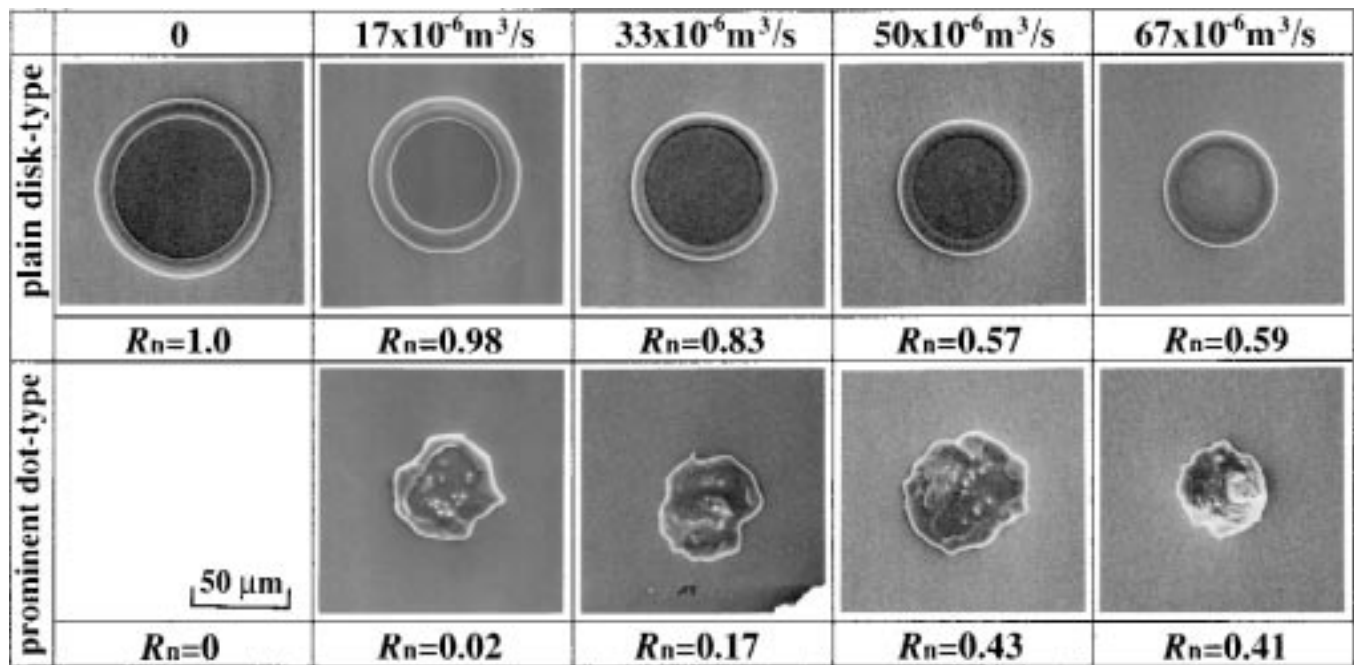


Fig. 8 SEM micrographs showing titanium splat morphology sprayed with different amounts of added nitrogen to plasma gas (particle size:  $32$  to  $38\ \mu\text{m}$ ).

### 3.5 Synthesis of In Situ Composite Coatings

The coatings sprayed with either titanium or aluminum particles less than  $32$  to  $38\ \mu\text{m}$  in diameter and a nitrogen ( $17 \times 10^{-6}\ \text{m}^3/\text{s}$ ) mixed plasma flame are TiN/Ti or AlN/Al *in situ* composites, respectively. The formation of TiN and AlN occurs during flight and on the substrate. Typical cross-sectional optical micrographs of the coatings sprayed with premixed titanium and aluminum and TiAl compound powder are shown in Fig. 10. The microstructure is characterized by a wavy layered structure.

Spectroscopic analyses of nitrogen content in coatings were performed; Fig. 11 shows the nitrogen content in coatings sprayed with titanium, aluminum, premixed titanium and aluminum, and TiAl compound powder. Titanium nitride is formed if the average particle size of titanium is smaller than  $38\ \mu\text{m}$ , although the coatings tend to be porous with fine titanium powder. The nitrogen content in the TiN/Ti composite coatings increases as the titanium powder becomes finer. In contrast, the coatings with aluminum powder form AlN/Al composite; i.e., the nitriding reaction occurs readily compared to the other powders. It is also notable that the nitrogen content in the coatings sprayed with premixed titanium and aluminum is much higher than that with TiAl compound powder.

The effect of nitrogen on the nitrogen content in coatings is shown in Fig. 12, in which the coatings were sprayed with pre-

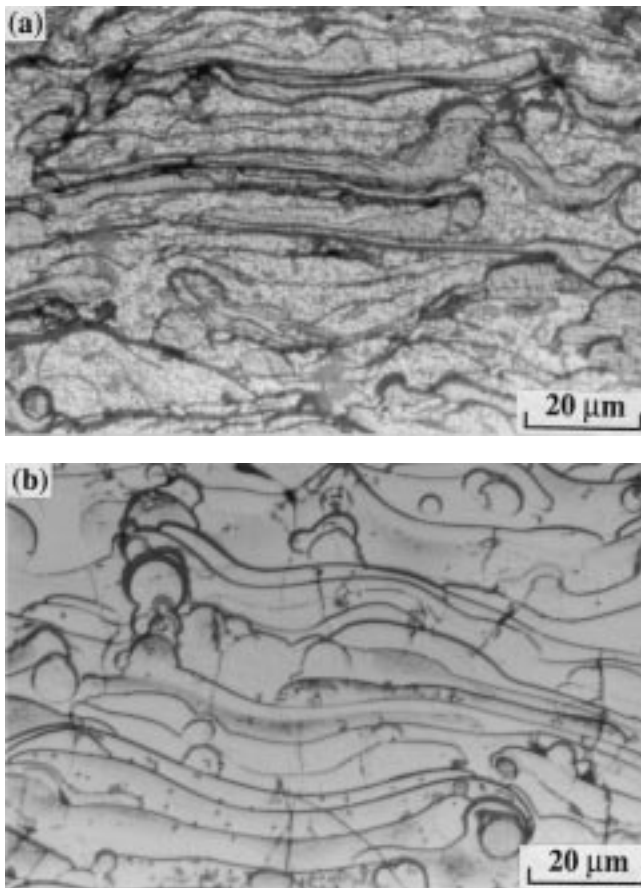


Fig. 10 Optical micrographs of coatings sprayed with (a) premixed Ti/Al powder and (b) TiAl compound powder (particle size:  $32$  to  $38\ \mu\text{m}$  and nitrogen mixed plasma gas (added  $\text{N}_2$ :  $17 \times 10^{-6}\ \text{m}^3/\text{s}$ ).

mixed titanium and aluminum and TiAl compound powder. An increase in nitrogen content occurs as the amount of mixed nitrogen is increased, although high amounts of mixed nitrogen make the coatings porous. We can find higher nitrogen content in the coatings with premixed titanium and aluminum powder at a given amount of added nitrogen than that with TiAl compound powder.

In order to identify the synthesized phases in the coatings sprayed with premixed titanium and aluminum powder, XRD patterns were taken with  $\text{Co } K_{\alpha}$  radiation. The coatings are composed of aluminum, titanium, TiN,  $\text{Ti}_2\text{N}$ , and AlN, which are not intermetallic matrix *in situ* composites, but the synthesis of TiAl and complex nitrides such as  $\text{Ti}_2\text{AlN}$  is incomplete.

If the substrate is preheated at  $873\ \text{K}$ , then intermetallic matrix *in situ* composite coatings can be formed, as is observed in conventional DC plasma spraying.<sup>[7,8,14]</sup> Since the mutual collisions of titanium and aluminum droplets are negligible during the flight, the formation of TiAl and  $\text{Ti}_2\text{AlN}$  definitely occurs on

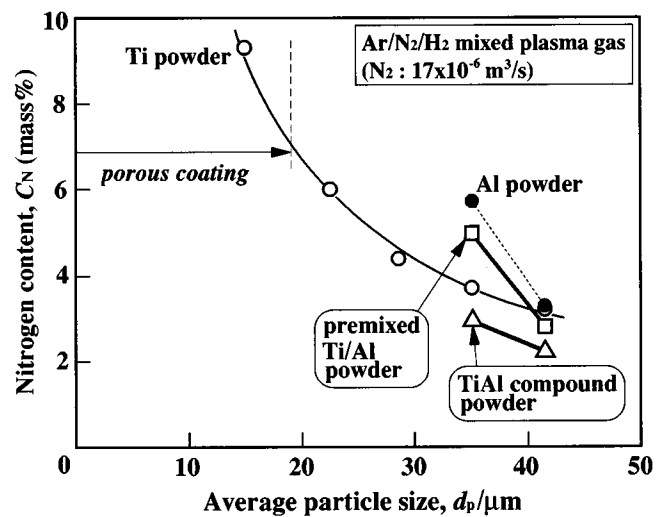


Fig. 11 Change in nitrogen content in coatings sprayed with various spray materials as a function of average particle size.

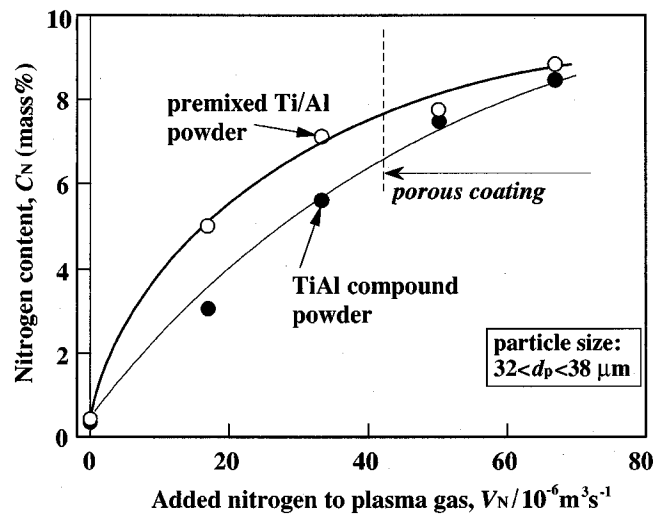
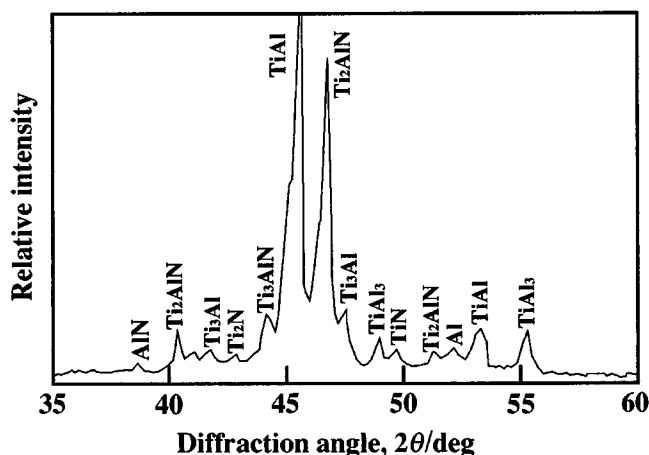
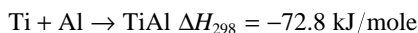


Fig. 12 Change in nitrogen content in coatings sprayed with different spray materials as a function of added nitrogen to plasma gas.



**Fig. 13** Typical XRD pattern of coating surface sprayed on preheated substrate at 873 K with premixed Ti/Al powder (32 to 38  $\mu\text{m}$ ) and mixed plasma gas (added  $\text{N}_2 = 17 \times 10^{-6} \text{ m}^3/\text{s}$ ).

the preheated substrate. The formation of TiAl is an exothermic reaction,<sup>[15]</sup>



Then, once the reaction of TiAl formation initiates, it progressively continues along with  $\text{Ti}_2\text{AlN}$  formation, as shown in Fig. 13 of the XRD pattern, in which the substrate has been preheated at 873 K just before spraying. Hence, premixed titanium and aluminum powder as a spray material is suitable to form intermetallic matrix *in situ* composites, which contrasts with expensive TiAl compound powder.

#### 4. Conclusions

Splats were collected on a stainless steel substrate to examine if nitrides were formed on metal droplets during flight in reactive RF plasma spraying. Change in splat morphology due to nitrogen absorption or nitride formation was elucidated. The effect of spray materials on the nitriding reaction was also discussed. The following results were obtained.

- With nitrogen ( $17 \times 10^{-6} \text{ m}^3/\text{s}$ ) mixed plasma and powders of 32 to 38  $\mu\text{m}$  in size, the splat morphology of titanium and TiAl is nearly circular in shape with an outer peripheral fringe, but aluminum has two morphologies: a disk type with an irregular periphery and a semimodular type.

- Titanium, aluminum, and TiAl droplets synthesize TiN or AlN not only during the flight in a nitrogen mixed plasma flame, but also on a substrate. The former mechanism is dominant at a higher nitrogen partial pressure in plasma gas and finer supplied particles.
- The coatings with premixed titanium and aluminum powder contain higher nitrogen than that with TiAl compound powder. A high substrate temperature is necessary to synthesize intermetallic matrix composite coatings.

#### Acknowledgment

Financial support by the Grants-in-Aid for Scientific Research from the Ministry of Education, Science, Sports and Culture (No. 09450280) for the present research is gratefully acknowledged.

#### References

1. J.C. Rawers, W.R. Wrzesinski, E.K. Roub, and R.R. Brown: *Mater. Sci. Technol.*, 1990, vol. 6, pp. 187-91.
2. M. Saqib, I. Weiss, G.M. Mehrotra, E. Clevenger, A.G. Jackson, and H.A. Lipsitt: *Metall. Trans.*, 1991, vol. 22A, pp. 1721-28.
3. J.D. Bryant, S.L. Kampe, P. Sadler, and L. Christodoulou: *Metall. Trans.*, 1991, vol. 22A, pp. 2009-19.
4. Y. Tsunekawa, M. Okumiya, N. Mohri, and I. Takahashi: *Mater. Sci. Eng.*, 1994, vol. A174, pp. 193-98.
5. D.J. Wortman, B.A. Nagaraj, and E.C. Duderstadt: *Mater. Sci. Eng.*, 1989, vol. A121, pp. 433-40.
6. Y. Tsunekawa, H. Harada, M. Okumiya, and I. Niimi: *J. Jpn. Inst. Met.*, 1990, vol. 54 (11), pp. 1256-60 (in English and Japanese).
7. Y. Tsunekawa, Y. Kohno, M. Okumiya, and I. Niimi: *J. Jpn. Inst. Light Met.*, 1991, vol. 41 (3), pp. 164-69 (in English and Japanese).
8. Y. Tsunekawa, K. Gotoh, M. Okumiya, and N. Mohri: *J. Thermal Spray Technol.*, 1992, vol. 1, pp. 223-29.
9. T.S. Srivatsan and E.J. Lavernia: *J. Mater. Sci.*, 1992, vol. 27, pp. 5965-81.
10. Y. Tsunekawa, M. Okumiya, K. Gotoh, T. Nakamura, and I. Niimi: *Mater. Sci. Eng.*, 1992, vol. A159, pp. 253-59.
11. Y. Tsunekawa, M. Okumiya, K. Kobayashi, M. Okuda, and M. Fukumoto: *J. Thermal Spray Technol.*, 1996, vol. 5(2), pp. 139-44.
12. M. Fukumoto, S. Katoh, and I. Okane: in *Thermal Spraying, Current Status and Future Trends*. A. Ohmori, ed., High Temperature Society, Kobe, Japan, 1995, pp. 353-58.
13. E.A. Brandes and G.B. Brook: *Smithells Metal Reference Book*, 7th ed., Butterworth Heinemann, Oxford, United Kingdom, 1992, pp. 14-17.
14. Y. Tsunekawa, M. Okumiya, M. Okuda, and M. Fukumoto. in *Surface Modification Technologies XI*, T.S. Sudarshan, M. Jeandin, K.A. Khor, eds., The Institute of Materials, London, 1998, pp. 234-45.
15. O. Kubaschewski and C.B. Alcock: *Metallurgical Thermochemistry*, 5th ed., Pergamon, Oxford, United Kingdom, 1979, pp. 316.